Fiber-taper coupling to Whispering-Gallery modes of fluidic resonators embedded in a liquid medium

Mani Hossein-Zadeh, and Kerry J. Vahala

Thomas J. Watson Laboratory of Applied Physics, California Institute of Technology, Pasadena, California 91125 USA
mhz@caltech.edu, www.vahala.caltech.edu

Abstract: We demonstrate efficient coupling to the optical Whispering-Gallery (WG) modes of a fluidic resonator consisting of a droplet embedded in a liquid medium. Unlike previous experiments the droplet is not levitated in an optical or electrostatic trap and free space coupling is replaced by phase-matched, waveguide coupling using a fiber-taper. We have observed critical coupling to fundamental WG modes of a 600 μm diameter water droplet at 980 nm. The experimental challenges towards making, stabilizing and coupling to the droplet resonators are addressed in this paper.

OCIS codes: (230.5750) Resonators; (230.0230) Optical devices; (999.9999) Optofluidics.

References and links

1. K. Campbell, A. Groisman, U. Levy, L. Pang, S. Mookherjea, D. Psaltis, and Y. Fainman, "A microfluidic 2×2 optical switch," Appl. Phys. Lett. **85**, 6119-6121 (2004).
2. D. V. Vezenov, B. T. Mayers, R. S. Conroy, G. M. Whitesides, P. T. Snee, Y. Chang, D. G. Nocera, and M. G. Bawendi, "A low-threshold high-efficiency microfluidic waveguide laser," J. Am. Chem. Soc. **25**, 8952-8953 (2005).
3. D. V. Vezenov, B. T. Mayers, D. B. Wolfe and G. M. Whitesides, " Integrated fluidic lightsource for optofluidic applications," Appl. Phys. Lett. **86**, 041104 (2005).
4. D. Psaltis, SR Quake, CH Yang, "Developing optofluidic technology through the fusion of microfluidics and optics," Nature **442**, 381-386 (2006)
5. A. Ashkin and J. M. Dziedzic, "Observation of resonances in the radiation pressure on dielectric sphere," Phys. Rev. Lett. **38**, 1351-1354 (1977).
6. H. –M. Tzeng, K. F. Wall, M. B. Logng, and R. K. Chang, "Laser emission from individual droplets at wavelengths corresponding to morphology-dependent resonances," Opt. Lett. **9**, 499-501 (1984).
7. R. Symes, R. M. Sayer and J. P. Reid, "Cavity enhanced droplet spectroscopy: principles, perspectives and prospects," Phys. Chem. Chem. Phys. **6**, 474-487 (2004).
8. S. –X Qian, J. B. Snow, and R. K. Chang, "Coherent Raman mixing and coherent anti-stokes Raman scattering from individual micrometer-size droplets," Opt. Lett. **10**, 499-501 (1985).
9. M. D. Barnes, K. C. Ng, W. B. Whitten, and M. Ramsey, "detection of single Rhodamine 6G molecules in levitated microdroplets," Anal. Chem. **65**, 2360-2365 (1993).
10. H. Azzouz, L. Alkhafadiji, S. Balslev, J. Johansson, N.A. Mortensen, S. Nilsson, A. Kristensen, "Levitated droplet dye laser," Opt. Express **14**, pp. 4374-4379 (2006)
11. AA Darhuber, JP Valentino, SM Troian, S. Wagner, "Thermocapillary actuation of droplets on chemically patterned surfaces by programmable microheater arrays" J. Microelectromech. Syst. **12**, 873-879 (2003)
12. JP Valentino, SM Troian, S Wagner, "Microfluidic detection and analysis by integration of thermocapillary actuation with a thin-film optical waveguide" Appl. Phys. Lett. **86**, 184101 (2005).
13. DB Wolfe, DV Vezenov, BT Mayers, GM Whitesides, RS Conroy, MG Prentiss, "Diffusion-controlled optical elements for optofluidics" Appl. Phys Lett. **87**, 181105 (2005)
14. R. J. Hopkins, L. Mitchem, A. D. Ward, and J. P. Reid, "Control and characterization of a single aerosol droplet in a single-beam gradient-force optical trap," Phys. Chem. Chem. Phys. **6**, 4924-4927 (2004).
15. M. Tona, and M. Kimura, "Parallel-plate ion trap useful for optical studies of microparticles," Rev. of Sci. Instrum. **75**, 2276-2279 (2004).
16. J. C. Night, G. Cheung, F. Jacques, and T.A. Birks, "Phase matched excitation of Whispering-Gallery mode resonances," Opt. Lett. **22**, 1129-1131 (1997).

#74477 - $15.00 USD Received 28 August 2006; revised 13 October 2006; accepted 15 October 2006

17. M. Cai, O. Painter, and Kerry J. Vahala, "Observation of critical coupling in a fiber-taper to silica-microsphere Whispering-Gallery mode system," Phys. Rev. Lett. **85**, 74-77 (2000).
18. Note that the thickness of a liquid-liquid interface is usually characterized by an interfacial 90-10 width (the distance required for the surrounding liquid density to drop from 90% to 10% of its bulk value). Usually 90-10 width for a water-oil liquid is smaller than 1 nm and therefore the surface of a droplet in the cladding medium is extremely smooth. (see D. M. Mitrinovic *et al*., "X-ray reflectivity study of the water-hexane interface," J. Phys. Chem. B **13**, 1779-1782 ,1999)
19. G. M. Hale, and M. R. Querry, "Optical constants of water in the 200-nm to 200 μm wavelength region," Appl. Opt. **12**, 555-563 (1973).
20. Cargille Laboratories: Refractive index liquid Series AAA 1.3 (background liquid), and immersion liquid code OHZB n = 1.4 (optical liquid)
21. B. E. Little, J. –P. Laine, and H. A. Haus, "Analytical theory of coupling from tapered fibers and half-blocks into microsphere resonators," J. Lightwave Technol. **17**, 704-715 (1999).
22. D. K. Armani, T. J. Kippenberg, S. M. Spillane and K. J. Vahala, "Ultra-high-Q toroid microcavity on a chip," Nature **421**, 925-929 (2003)
23. C. Yamahata, C. Lotto, E. Al-Assaf, M. A. M Gijs, "A PMMA valveless micropump using electromagnetic actuation," Microfluidics and Nanofluidics **1**, 197-207 (2005)
24. S. Schiller, and R. L. Byer, "High-resolution spectroscopy of whispering-gallery modes in large dielectric spheres," Opt. Lett. **16**, 1138-1140 (1991).
25. V. Vassiliev, V. Velichansky, V. S. Ilchenko, M. L. Gorodetsky, L. Hollberg, A. V. Yarovitsky, "Narrow-line-width diode laser with a high-Q microsphere resonator," Opt. Commun. **158**, 305-312 (1998).
26. S. Arnold, M. Khoshsima, I. Teraoka, S. Holler, and F. Vollmer, "Shift of whispering-gallery modes in microspheres by protein absorption," Opt. Lett. **28**, 272-274 (2003).
27. A. M. Armani, and K. J. Vahala, "Heavy water detection using ultra-high-Q microcavities," Opt. Lett. **31**, 1896-1898 (2006).
28. F. Mugele and J. C. Baret, "Electrowetting: From basics to applications," J. Phys.-Cond. Matt. **17**, 705-774 (2005)

1. Introduction

Optofluidics is an emerging technology that seeks to integrate photonic with fluidic devices and may lead to powerful new tools for a broad range of applications in photochemistry, photobiology and sensor design [1-4]. Optical Whispering-Gallery (WG) resonators are among the most versatile of photonic devices, finding applications as lasers, filters, sensors, and oscillators; and fluidic versions of these resonators based on liquid micro-droplets were studied some 20 years ago and shown to exhibit ultra-high-*Q* factors, owing to surface-tension-induced smoothing of the WG dielectric interface [5,6]. The combination of high-*Q* and a micro-scale mode volume creates an ideal environment for study of numerous physical phenomena, including cavity-enhanced spectroscopy (CRM, SRS, CARS) [7], study of nonlinear properties of liquids [8], sensors [9], and demonstration of laser operation in liquids [6,10]. Unfortunately, droplets also suffer from several practical limitations, including the complexity associated with manipulating and controlling droplet structures as well as highly inefficient optical coupling to and from the droplet resonator. Within the context of optofluidics [4], new manipulation and control methodologies have emerged that could one day address the former of these challenges [11-13]. Concerning the latter point, free space excitation of droplets has been the only method employed to date. This not only presents severe limitations in terms of phase matching considerations to the optical WG resonators, but, typically, leads to poor spatial overlap with the excitation wave and the optical mode. This paper addresses several key limitations of using fluidic-based optical resonators. First, the stability of fluidic resonator itself is addressed by embedding the resonator liquid in a second, "cladding" liquid. This prevents evaporation, and hence stabilizes spectra. Second, a highly efficient, waveguide-based coupling is demonstrated using a fiber-optic taper waveguide.

Efficient optical coupling to WG modes and droplet stabilization are the main challenges toward optical characterization of droplets. Generally a Guassian laser beam excites WG modes of a droplet and a broad area detector collects the scattered light. Free space coupling to a Gaussian beam is very inefficient due to the phase mismatch and minuscule spatial

#74477 - $15.00 USD Received 28 August 2006; revised 13 October 2006; accepted 15 October 2006

overlap between the pump field and the circulating WG modes. The input optical beam is usually scattered by stationary droplets immobilized in an optical [10,14] or electrostatic [15] trap, or moving droplets in a stream generated by a vibrating orifice aerosol generator [8]. Generally moving droplets have distorted shapes and also coupling to them introduces a very short interaction time (the time it takes the molecule to transit the probe volume defined by the pump laser). Static techniques enable continuous wave operation, but they require special experimental arrangements to trap the droplet and overcome the time-dependence of resonator size due to evaporation [14].

Here we demonstrate a novel and simple method for stabilization and efficient optical coupling to a droplet resonator. In our approach the droplet is embedded in a liquid medium with a refractive index lower than that of the droplet and the optical coupling is achieved using a standard fiber-taper coupler [16,17]. This method is equivalent to the phase-matched waveguide coupling to a microdisk resonator, which is currently used in integrated photonic devices. We show that with careful design, critical coupling to average size (500-1000 μm diameter) droplet resonators is achievable. Thereby the coupling efficiency (both to and from the droplet) is boosted by many orders compared to free-space methods.

2. Droplet resonator

Making droplets and stabilizing them is a major challenge for optical experiments with droplets and microdroplets. Although surface tension generates a near spherical shape with exceptional smoothness, contact with most solid surfaces can result in complete deformation to a dome shaped droplet that is unable to support WG modes. Free flying and levitated droplets can preserve their near-spherical shape due to elimination of physical contact but have the disadvantages noted above. Here, there is an attempt to simplify the experimental arrangement and enable the possibility of using fiber-taper coupling to droplets.

In our experiment the droplet is immersed in an immiscible liquid "cladding" medium. In this environment the droplet maintains its shape and size for a prolonged period of time while being protected from external contaminants (we have not observed any noticeable change in the physical and optical properties of the droplet resonator even after leaving it inside the background liquid for periods as long as a week). Due to the smoothness of the water-cladding interface the scattering loss is negligible and the optical loss is dominated by the absorption and radiation loss [18].

Also the surrounding liquid acts as a damping force for the mechanical vibrations of the droplet and improves the mechanical stability of the resonator. To achieve optical resonance in a droplet its refractive index must be larger than that of the surrounding medium and in the same time the two liquids must be immiscible. Simultaneous fulfillment of these conditions is the main disadvantage of this technique and sets a limit on the variety of liquid pairs that can serve as medium and resonator.

Table 1. Important physical and optical (λ = 980 nm) properties of liquids used in the experiment [19,20].

Liquid	α (cm^{-1})	n	ρ (g/cm^3)	σ (dynes/cm)
Water	0.43	1.326	1	73
Background liquid	0.001	1.297	1.940	18

The liquid medium in our experiment is an index matching optical liquid with a refractive index of 1.3, which we refer to it as the cladding liquid. This liquid is insoluble in water, its density is about 2 times water density and it has very low optical loss within a wide optical spectrum (λ = 360-1300 nm). Our droplet resonators are made of water. Water is very lossy around λ =1550 nm so to operate in relatively high-*Q* regime the experiments are performed at λ =980 nm (see Table 1).

Due to radiation loss the magnitude of the index contrast can be a limiting factor for the droplet size. Figure 1 shows the calculated radiation limited quality factor (Q_{rad}) at λ = 980

#74477 - $15.00 USD Received 28 August 2006; revised 13 October 2006; accepted 15 October 2006

nm for a water droplet with perfect spherical shape embedded in a medium yielding an index contrast of 0.03 (the calculation is based on the model presented in Ref. 21 that uses the volume current method to approximate the radiation loss). Since the absorption loss limited quality factor (Q_{abs}) for water at this wavelength is 1.98×10^5 ($Q_{abs} = 2\pi n/\alpha\lambda$, α: linear loss factor, n: refractive index). The diameter of an *ideal* water droplet (D) can be as small as 0.25 mm and still operate in the absorption loss limited regime in our background liquid (at D = 0.25 mm and $\lambda = 980$, Q_{rad} is about 2.3×10^5).

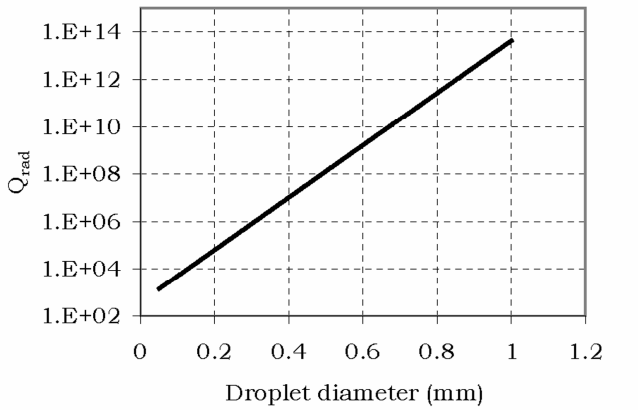

Fig.1. Calculated radiation limited quality factor at λ = 980 nm for the fundamental Whispering-Gallery resonance of a water sphere embedded in a medium with an index contrast of 0.03.

Notice that the measured quality factor is the total (or loaded) quality factor of the resonator, Q, which can be decomposed into several components:

$$\frac{1}{Q} = \frac{1}{Q_{ext}} + \frac{1}{Q_{abs}} + \frac{1}{Q_{rad}} \tag{1}$$

Here we have assumed that due to smoothness provided by surface tension, the scattering loss is negligible. Q_{ext} is the external quality factor (produced by waveguide coupling), Q_{rad} is the radiation limited quality factor, and Q_{abs} is the absorption loss limited quality factor that can be written as:

$$Q_{abs} = \frac{2\pi n_{eff}}{(F_r\alpha_r + F_m\alpha_m)\lambda_0} \tag{2}$$

Here n_{eff} is the effective refractive index of the WG mode. F_r and F_c are the fractions of optical power circulating inside the droplet resonator and in the cladding medium (evanescent field) respectively. These fractions can be estimated by calculating the radial dependence of the E-field for the associated WG mode. Q_{ext} is the Q-factor associated with losses due to external coupling and can be approximated as [21]:

$$Q_{ext} = \frac{m\pi}{\kappa^2} \tag{3}$$

where κ is the optical coupling factor and m is the azimuthal mode order.

The liquid cladding eliminates evaporation, but still a mechanism is required to immobilize the droplet. Adhesion to a stable object is the simplest way of trapping a droplet but usually it spoils the symmetrical shape required to support WG traveling waves. Since surface tension and the shape of the trapping object governs the shape of the droplet, an object with the same symmetrical properties sought after in the resonator might be the suitable choice. A silica sphere is an ideal trapping object that preserves the optical resonant properties while trapping the droplet. Figure 2 shows the schematic diagram of a droplet trapped on top of a silica sphere in the cladding liquid.

#74477 - $15.00 USD Received 28 August 2006; revised 13 October 2006; accepted 15 October 2006

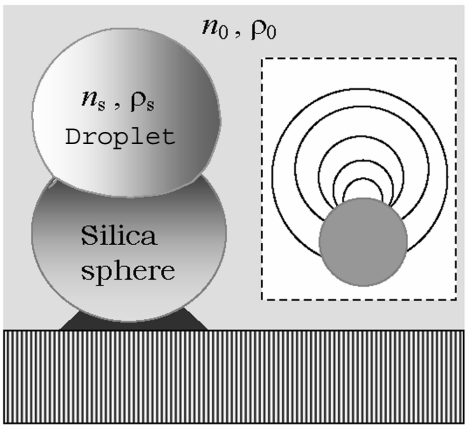

Fig. 2. Stabilizing the droplet using a silica sphere. The adhesion force between water and silica traps the droplet. Based on experimental results if $\rho_0 \approx 2\times\rho_s$ ($\Delta\rho \approx \times\rho_s$) and the diameter of the droplet is equal to that of the silica sphere, the final shape is close to a perfect sphere. Inset shows the qualitative behavior of the droplet shape and size.

Deriving an analytic expression for the shape of the droplet is a difficult task and beyond the scope of this paper. However as an insight into the overall behavior of the droplet shape, we use a phenomenological analysis based on experimental observations and the forces involved in the system. Four major forces determine the stability and the shape of the droplet: buoyant force, droplet weight, surface tension (σ), and the adhesive force between silica and water (since silica is hydrophilic). Although the first two forces are constant for a given droplet volume and $\Delta\rho$ ($=\rho_0-\rho_s$), the last two forces depend on droplet shape. The equilibrium value of the contact area between silica and water and the equatorial curvature (eccentricity) of the droplet balance all these forces. Experimental observations show that when $\Delta\rho \approx \rho_s$ (and the diameter of the droplet (D) is equal to that of the silica sphere, the final shape is close to a perfect sphere with a small eccentricity (the semi-minor axis is in the equatorial plane so the droplet is prolate). Droplets that have larger diameters than the silica sphere have larger eccentricity. The inset in Fig. 2 shows the qualitative behavior of the droplet shape as its volume changes.

3. Fiber-taper coupling to WG modes of a droplet

As was pointed out earlier, so far, free-space coupling using a Guassian beam has been the preferred method for exciting the WG modes of droplets. On the other hand evanescent coupling from a fiber-taper has become the preferred technique for exciting the WG modes inside silica microspheres [16,17] and more recently microtoroids [22]. Experimental results have shown highly efficient coupling to silica microspheres through a taper-to-sphere junction [17] but, to our knowledge, this method has not been used for coupling to droplet resonators. Two, key requirements for efficient coupling between a fiber-taper and a spherical resonator are phase matching and sufficient overlap between the evanescent electromagnetic fields. In our experiment the index contrast between the resonator and the surrounding medium is low so the penetration depth of evanescent fields and therefore the overlap is improved compared to previous cases (where the background medium was air); however, phase-matching needs more attention.

Each WG mode is identified with three indices l, m and q (for polar, azimuthal and radial mode orders) and its polarization (TE or TM). It is well known that in an ideal spherical resonator WG modes possess a $2l+1$ degeneracy with respect to the azimuthal mode number m ($l \geq m \geq -l$), so the resonant frequencies are determined by l and q. Also, the value $l-m+1$ is equal to the number of field maxima in the polar direction (perpendicular to the equatorial plane).

#74477 - $15.00 USD Received 28 August 2006; revised 13 October 2006; accepted 15 October 2006

The effective index of the WG modes inside a spherical resonator can be estimated using the characteristic equation presented in Ref. 21:

$$\left(\eta_s \alpha_s + \frac{l}{R}\right) j_l(kn_s R) = kn_s j_l'(kn_s R) \qquad (4)$$

where

$$\eta_s = \begin{cases} 1 & \text{TE modes} \\ \dfrac{n_s^2}{n_0^2} & \text{TM modes} \end{cases} \qquad \text{and} \qquad \alpha_s = \sqrt{R^{-2} l(l+1) - k^2 n_0^2}$$

k is the propagation constant, R is the sphere radius, n_o and n_s are the refractive index of the cladding and the sphere respectively, and j_l is the Spherical Bessel function of the l-th order. The calculated value of the effective refractive index for the fundamental TM polarized WG mode ($l = m$, $q = 1$) of an average size ($D \sim 0.3 - 1$mm) spherical water resonator in the cladding liquid is within 1.3192 and 1.3145 at $\lambda = 980$ nm (The upper and lower limits correspond to resonance in a droplet with a diameter of 1 mm and 0.3 mm respectively). Figure 3 shows the calculated effective refractive index of the fundamental mode of a fiber-taper in the cladding liquid as a function of taper diameter at $\lambda = 980$ nm.

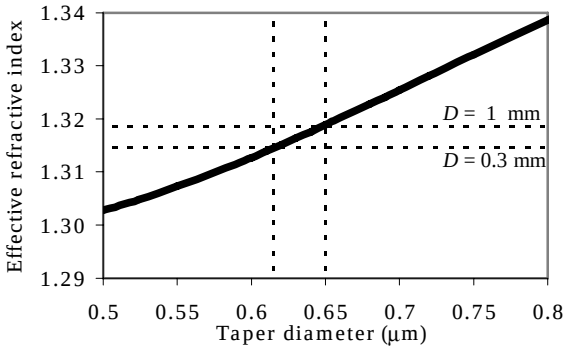

Fig. 3. Calculated effective refractive index of a cylindrical dielectric waveguide made of silica in a medium with $n_o \approx 1.3$, at $\lambda = 980$ nm. The dashed lines indicate the near phase-matched coupling regime for a water droplet ($D = 0.3 - 1$ mm).

This effective refractive index of the fiber-taper is estimated by solving Maxwell equations for a step-index cylindrical waveguide and deriving the propagation constant of the HE11 mode using proper boundary conditions [21]. The dashed lines in Fig. 3 indicate the near phase-matched coupling regimes for a water droplet ($D = 0.3 - 1$mm), at $\lambda = 980$ nm. As one may see, the optimal taper diameter is between 600 to 650 nm.

4. Fiber-taper coupling to WG modes of a droplet

Fig. 4 shows a schematic diagram of the experimental configuration used for coupling the fiber-taper to the droplet in a liquid medium. The silica sphere trap is glued (using Epoxy) to a steel base and is placed in a glass container filled with the background liquid. The droplets are made by forming a mist of small droplets using a syringe. We use a fiber-tip to capture a single droplet from the mist and transfer it to the trap in the background liquid. The size of the syringe, injection speed and the diameter of the fiber-tip determine the size of the captured droplets. We were able to generate droplets with diameters between 100-1000 μm with relatively good yield. To control the droplet size with high accuracy one can use micropumps that are capable of working at flow rates as low as 200 μl/min [23]. The fiber-taper is formed

#74477 - $15.00 USD Received 28 August 2006; revised 13 October 2006; accepted 15 October 2006

by heating and stretching a length of single mode fiber and then mounted on a U-shape holder using epoxy.

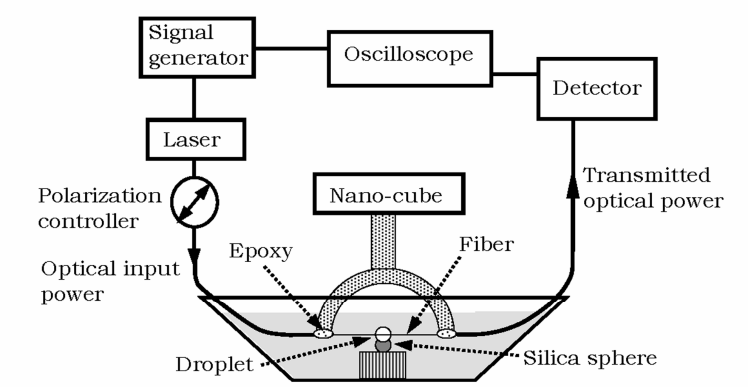

Fig. 4. Schematic diagram of the experimental configuration

Note that the cladding liquid does not interact with steel, epoxy and water. Therefore, the traps and the fiber-taper holder can be immersed in the liquid without changing its chemical and optical properties. The position of the fiber-taper is controlled and monitored with a resolution of 1 nm using three closed loop controlled piezomotors (manicure). Two CCD cameras monitor the relative taper-droplet position from side and top.

The laser source is a tunable single mode laser with a linewidth of 300 kHz. In order to measure the transmission spectrum of the taper-droplet junction we modulate the laser wavelength and detect the transmitted optical power with an amplified PIN photodetector and an oscilloscope. The polarization of the optical input field is controlled by an in-line polarization controller between the laser and fiber-taper. Note that since the resonant wavelengths of the TE and TM polarized WG modes are slightly different, the polarization controller and the transmission spectrum can be used to evaluate the polarization state of the WG modes circulating within the droplet. In our experiments the polarization controller is always tuned for optimal coupling to TM polarized WG modes. In all experiments the optical input power to the fiber-taper is 1 mW (however, all the presented transmission spectrums are normalized to the non-resonant transmission case).

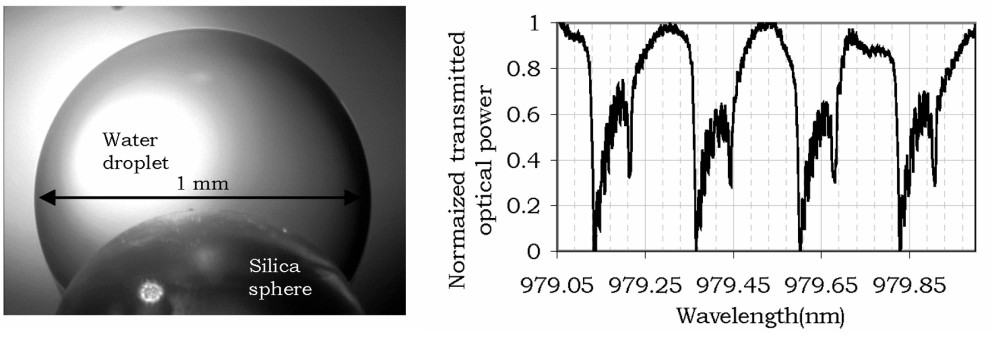

(a) (b)

Fig. 5. (a) A water droplet trapped on top of a silica sphere inside the background liquid. Because of the transparency of the droplet the contact margin in the front is not visible. (b) Transmission spectrum of a fiber-taper coupled to the water droplet (D = 1 mm). The TM polarized fundamental modes ($l = m$, q =1) are critically coupled. The measured $\Delta\lambda_{FSR}$ = 0.23 nm is in very good agreement with the calculated value (0.232 nm) using the effective refractive index for the TM (4227,4227,1) mode.

#74477 - $15.00 USD Received 28 August 2006; revised 13 October 2006; accepted 15 October 2006

Figure 5(a) shows the photograph of a water droplet trapped by a silica sphere with a diameter of 1 mm. The droplet diameter is equal to that of the silica sphere and exhibits a small eccentricity, which removes the degeneracy of the azimuthal ($l \neq m$, q =1) modes. Fig. 5(b) is the measured TM transmission spectrum of a fiber-taper coupled to the water droplet shown in Fig. 5(a). The measured free-spectral-range, $\Delta\lambda_{FSR}$ = 0.23 nm, is in very good agreement with the calculated value (0.232 nm) using the effective refractive index for the TM mode (l = 4227, m = 4227, q = 1) and measured diameter using the photograph. Although the coupling strength of the azimuthal modes decreases as l-m increases, in the transmission spectrum we can see two extra modes after the 7th azimuthal mode, each with relatively large coupling factors. Numerical analysis shows that these modes have resonant frequencies very close to those of TM (4169,4169,4) and TM (4204,4204,2) modes. Coupling to these modes may be explained by the fact that the penetration depth of the evanescent E-field in the surrounding medium increases with q (radial mode order).

Figure 6(a) shows the TM transmission spectrum of the droplet in the vicinity of a fundamental mode. *Even* azimuthal modes up to l-m = 12 are visible in this spectrum.

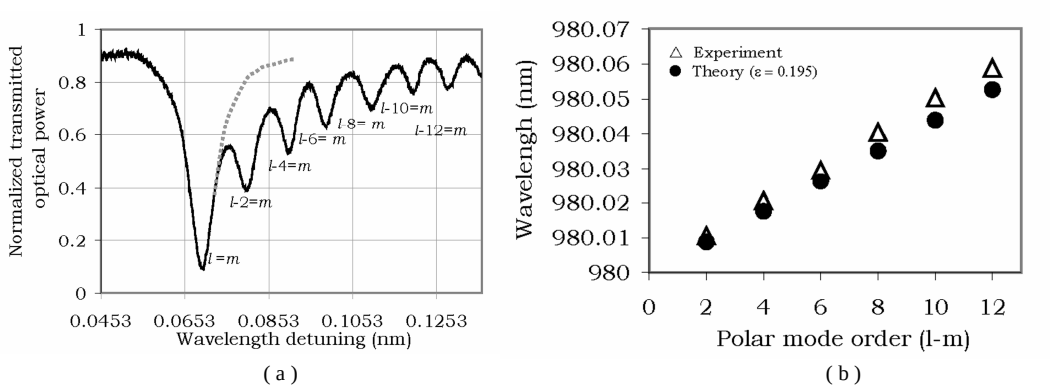

Fig. 6. (a) Measured transmission spectrum of the fiber-taper coupled to a water droplet ($D \approx$ 1 mm) inside optical liquid ($n \approx$ 1.3) around λ = 980 μm. The main dip corresponds to the fundamental Whispering-Gallery resonance ($l = m$) and the small dips are azimuthal modes (l-m=2K, K is a nonzero integer). The resonant wavelengths of azimuthal modes are red shifted due to the positive eccentricity of the droplet (prolate form). The resonant wavelengths of these modes are separated by 0.0085 nm intervals. The dashed line is to guide the eye for the Lorentzian shape of the fundamental resonance which has a Q of 1.15×10^5. (b) Experimental (triangles) and calculated (dots) values of resonant wavelengths against azimuthal mode order (l-m).

It has been shown that in a spheroid resonator the wavelength spacing between a azimuthal mode and the fundamental mode is $(l\text{-}|m|)\delta\lambda_{ec}$ where $\delta\lambda_{ec}$ is given by [24,25].

$$\delta\lambda_{ec} = \pm\frac{\Delta\lambda_{FSR}\varepsilon^2}{2} \qquad \left(\varepsilon = \frac{\sqrt{a^2-b^2}}{a}\right) \tag{5}$$

The negative sign stands for an oblate spheroid, positive sign corresponds to a prolate (stretched) spheroid, and ε is the eccentricity of the spheroid. a and b are the equatorial and axial spheroid radius respectively. So the positive wavelength shift in Fig. 6(a) indicates that the droplet is prolate (a fact that can also be discerned from measurement of the photograph). Using equation 5 and an estimated value of 0.195 for ε (a and b are measured using the droplet photograph) we have calculated the resonant wavelengths of azimuthal modes. Fig. 6(b) shows the resonant wavelengths plotted against l-m. The triangles are the experimental data and the solid dots are the calculated values. Notice that since the fiber-taper is located in the equatorial plane *odd* azimuthal modes are not excited, so the spacing between the adjacent modes in Fig. 6(a) is $2\times\delta\lambda_{ec}$. The minor discrepancy between theoretical prediction and the experimental results is associated with non-ideal shape of the silica sphere that causes deviation from a spheroidal droplet shape.

#74477 - $15.00 USD Received 28 August 2006; revised 13 October 2006; accepted 15 October 2006

The transmission spectrums in Fig. 5(b) and 6(a) are measured while the coupling-gap was about 100 nm. We were not able to enter the over coupled regime because reducing the gap size would result in attachment of the fiber-taper and the droplet. The measured quality factor (Q) for the $l = m$ mode in Fig. 6(a) is 1.15×10^5. A theoretical estimation of Q can be obtained using equation 1,2,3 and 4. For a water droplet with a diameter of 1 mm in the cladding medium, $Q_{rad} = 5\times10^{11}$, $n_{eff} = 1.319$, $F_r \sim 0.9$ and $F_c \sim 0.1$. According to Fig. 6(a) the normalized transmitted power at the resonant wavelength of the $l = m$ (= 4227) mode is about 0.07 which corresponds to coupling factor of $\kappa = 0.26$. Using these values the estimated value of Q is 1.04×10^5 which is in very good agreement with the measured value (less than 1% difference).

In our second experiment we used a silica sphere with a diameter of 0.5 mm to trap a sub-millimeter droplet. Figure 7 shows the top-view (a) and side-view (b) of a water microdroplet with a diameter of about 600 μm coupled to a fiber-taper.

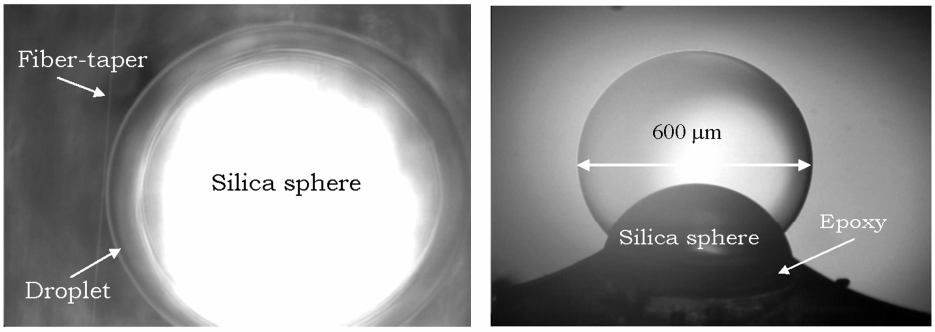

Fig. 7. A water microdroplet with a diameter of 600 μm coupled to a fiber-taper (a) Top-view and (b) Side-view. In the side-view picture the fiber-taper is not visible because the camera is focused on the great circle of the sphere.

Figure 8 shows the transmission spectrum of the fiber-taper coupled to the water microdroplet shown in Fig. 7 near $\lambda = 980$ nm. The measured free-spectral-range ($\Delta\lambda_{FSR}$) is 0.381 nm and again the fundamental modes are strongly coupled to the fiber-taper. Due to the small eccentricity, the resonant wavelengths of the azimuthal ($m \neq l$) modes are very close and cannot be resolved. The wavelength spacing between adjacent *even* azimuthal modes is about 0.0066nm corresponding to an eccentricity of $\varepsilon = 0.132$ (according to equation 5).

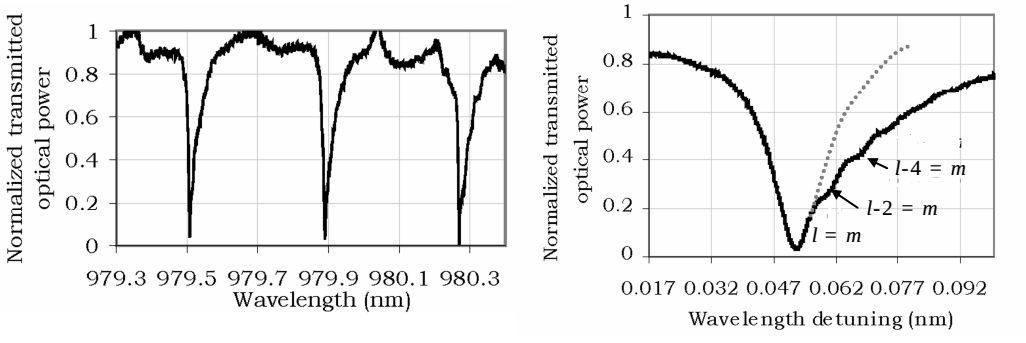

Fig. 8. (a) Measured optical transmission spectrum of the fiber-taper coupled to a water microdroplet (D = 600 μm) around λ = 980 nm. Due to small eccentricity the resonant wavelengths of azimuthal modes are very close and cannot be resolved. The $\Delta\lambda_{FSR}$ is 0.381 nm. (b) Transmission spectrum near resonance. The wavelength spacing between adjacent *even* azimuthal modes is about 0.0066 nm (The dashed line is to guide the eye for the Lorentzian shape of the fundamental resonance).

#74477 - $15.00 USD Received 28 August 2006; revised 13 October 2006; accepted 15 October 2006

The measured quality factor of the fundamental mode is 7.5×10^4 at critical coupling. The calculated value of Q at critical coupling (zero transmission at resonant wavelength of the $l = m$ mode) is 7.79×10^4 that is in very good agreement with the measured value (in this case $Q_{rad} = 3\times10^9$, $n_{eff} = 1.326$, $F_r \sim 0.85$, $F_c \sim 0.15$, $l = m = 2530$ and $\kappa = 0.26$). The smaller size of this droplet enabled the possibility of observing the overcoupled regime (The penetration depth of the evanescent-field is larger so overcoupling happens before the fiber-taper attaches to the droplet). The normalized transmitted optical power against taper-droplet separation (coupling-gap) is shown in Fig. 9.

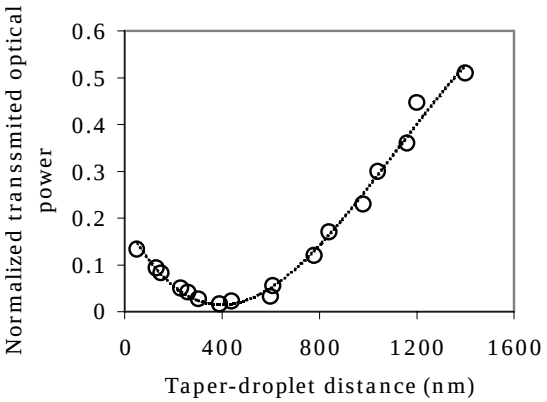

Fig. 9. Normalized transmission against taper-droplet separation (coupling gap) while the fiber-taper is coupled to the fundamental WG mode ($l = m$) of the droplet (λ ~980 nm). The dotted line is a polynomial fit to the experimental data.

The fiber-taper is coupled to the fundamental WG mode ($m = l$) of the droplet ($\lambda \sim 980$ nm). We should point out that all the experiments were performed on an optical table to isolate the system from the mechanical perturbations. We have not observed a considerable change in resonant wavelengths during our measurements (that usually takes 5 to 10 minutes). One of the principal sources of drift/fluctuation in resonators of all types is thermal fluctuation of the environment. We note that there is at least the potential to compensate this effect in liquid resonators by proper selection of resonator and cladding media.

5. Conclusion

We have demonstrated a novel technique for efficient optical coupling to WG modes of a droplet resonator immersed in liquid environment. The liquid environment not only stabilizes the droplet size but also enables the use of simple trapping mechanisms. Low index contrast between the resonator and the surrounding media combined with the unique geometry of the fiber-taper enables efficient coupling to WG modes of the droplet.

In a liquid medium with a refractive index of 1.3, we have observed critical coupling to WG modes of water droplets as small as 600 μm in diameter. An important issue that demands more effort is reducing the droplet size. The smallest droplet presented in this work has a diameter of 600 μm while previous works were mainly using microdroplets with diameters less than 100 μm. In principle one can trap microdroplets by employing silica microspheres. Due to the larger penetration depth of the evanescent field, coupling to smaller droplets is stronger for the same gap size but high-Q operation may demand larger index contrast to over come the radiation loss. A large coupling gap decreases the mechanical interaction between the droplet the taper resulting in a more stable coupling especially in the visible regime.

The applications of droplet Whispering-Gallery resonators can be as versatile as silica microspheres, microtoroids and other WG resonators. Specifically, droplet resonators are

#74477 - $15.00 USD Received 28 August 2006; revised 13 October 2006; accepted 15 October 2006

attractive for certain applications where an efficient interaction between light and a liquid is required. The general idea is that the interaction between the evanescent field and the liquid translates the optical properties of the liquid to the modal properties of a resonator immersed in that liquid (such as quality factor or resonant wavelength). Previously this principle has been exploited to detect molecules by immersing a optical WG resonator (microtoroid or microsphere) in the liquid under test [26,27]. The strength of interaction between the optical field and a liquid (therefore the sensitivity of the system) depends on the spatial overlap between the resonant optical field and the liquid as well as the quality factor of the resonator (Q). Usually a large percentage of the optical field circulates inside the resonator and only a small evanescent tail interacts with the surrounding medium. Since in a droplet resonator the optical mode resides inside the liquid under test the spatial overlap is larger compared to a solid resonator immersed in the same liquid. So assuming that the optical quality factors are identical the droplet resonator is more sensitive than the solid resonators.

One of the most important advantages of fluidic photonic devices is their active reconfigurability using various types of actuation [11,28]. In a droplet resonator this property manifests itself as the tunability of the diameter and eccentricity. Figure 10 shows two possible techniques for active control of the droplet eccentricity/diameter.

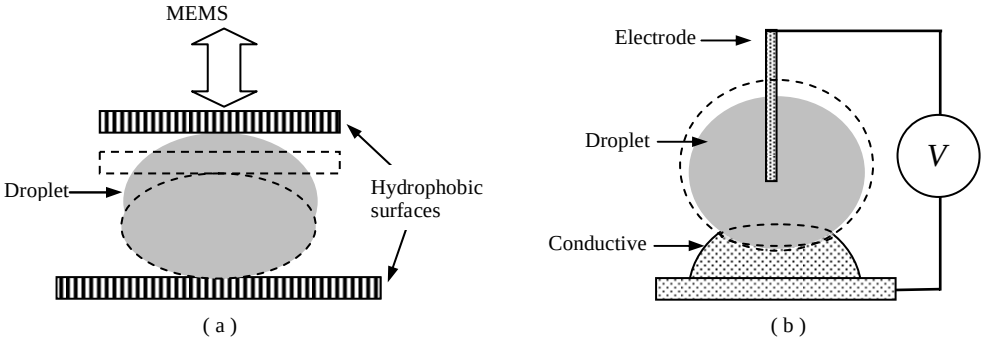

Fig. 10. (a) Mechanical tuning of the eccentricity/diameter of a droplet resonator sandwiched between two hydrophobic surfaces. (b) Electrical tuning of the eccentricity/diameter of a droplet resonator trapped on top of a silica hemisphere (using electrowetting effect [28]).

The first approach (Fig. 10(a)) uses hydrophobic surfaces combined with MEM actuation (piezoelectric or electrostatic) to control the eccentricity/diameter of a droplet sandwiched between two plates. In the second approach the droplet is trapped on top of a hemisphere mounted on a conductive surface and a microelectrode is inserted inside the droplet. The eccentricity/diameter can be controlled by changing the voltage applied on the electrode (V) through electrowetting effect [28]. Note that by tuning the droplet eccentricity/diameter one can control the wavelength of the resonant modes as well as the extension of the evanescent field in the liquid (and therefore the optical coupling factor). This feature can be beneficial in many applications specially sensor applications where matching the resonant wavelength with absorption lines of molecules is desired.

This work is the first attempt to make a liquid-phase replica of the fiber-taper coupled spherical resonators. Although, there remain many issues concerning the ultimate practicality of these devices, the ability to stably couple to a high-Q fluidic resonator with high efficiency suggests that these structures may have applications within the broader field of optofluidics. Along these lines, it is entirely possible that more planar liquid resonators could one day be developed. These would have additional advantages, including a simplified mode spectrum, as compared to spherical resonators. Finally, there is also the possibility that the taper waveguide itself could one day be replaced using a liquid filamentary waveguide. Such filamentary guides have already been demonstrated [2]. In this event, an all-fluidic resonator assembly would result.

#74477 - $15.00 USD Received 28 August 2006; revised 13 October 2006; accepted 15 October 2006